CHAPTER–1

Brief Introduction to Computational Chemistry

[1.1] Introduction

Historically, the area of chemistry mostly relies on experimental studies. However, over the last few decades, a number of sophisticated computational techniques have been developed which are being extensively used to solve various problems in chemistry. The modern computational technique uses different approximation schemes such as Hartree-Fock, post-Hartree-Fock, semiempirical or forcefield methods to tackle different chemical problems which are otherwise difficult to study experimentally. They are found to be extremely useful in studying reaction mechanisms, determining molecular geometries of ground and excited states, different electronic and spectroscopic properties etc. [1]. The tools that are used in computational chemistry can be divided into five broad categories [2] which are as follows-

(a) Molecular mechanics
(b) *Ab initio*
(c) Semiempirical method
(d) Molecular dynamics
(e) Density functional theory

Molecular mechanics (MM), which is suitable for studying larger systems, uses the law of classical mechanics to model molecular systems by considering the atoms as balls and the bonds as springs. On the other hand, both the Semiempirical (SE) and *Ab initio* methods rely on solving the Schrődinger wave equation to determine the energy and wavefunction of a molecule. Further, it is to be noted that the SE calculations are relatively slower than MM but considerably faster than *Ab initio* calculations. Molecular dynamics calculations employ the laws of motion to study a molecule whereas Density Functional Theory (DFT) calculations, unlike the wavefunction methods (SE and *Ab initio*) use the electron density of a system to describe its properties [3]. As all the works presented in this thesis were carried out by employing DFT calculations, therefore, a brief description of DFT is provided below.

[1.2] Density Functional Theory

DFT calculations do not involve the calculation of a wavefunction, rather it derives the electron density function denoted by $\rho(x, y, z)$ (where x, y and z are the spatial coordinates) to describe different properties of a many electron system. In other words, DFT calculations are the substitute for the complicated many electron wavefunction which

contains 3N variables (N is the number of electrons and each electron has three spatial variables). Therefore, it can be stated that, unlike the wave functional methods which need to consider a large number of 3N variables, DFT calculations deal with only three variables which is indeed, far easier to handle. DFT, which is now a leading method to calculate electronic structures in different key areas, is based on two formalisms put forwarded by Hohenberg and Kohn in 1964 [3c].

[1.2.1] The Hohenberg-Kohn Theorems

According to the first Hohenberg-Kohn theorem "the ground state electron density function $\rho_0(x, y, z)$ can be used to determine all the properties of a molecule in its ground state" [3c]. In other words, any ground state property is a functional (a functional is a function of another function) of $\rho_0(x, y, z)$. Therefore, the ground state energy (E_0) of a molecule can be represented as

$$E_0 = F[\rho_0(x, y, z)] \tag{1.1}$$

The relationship (1.1) indicates that ground state energy i.e. E_0 is a functional of $\rho_0(x, y, z)$.

The second Hohenberg-Kohn theorem states that "any trial electron density function will give an energy higher than (or equal to, if the trial wave function is exactly the true electron density function) the true ground state energy" [3c]. In DFT calculations, the electronic energy obtained from a trial electron density corresponds to the energy of the electrons moving under a potential imposed by the atomic nuclei. The potential imposed by the atomic nuclei is known as external potential ($\nu(r)$, where r is the position vector for the spatial coordinate (x, y, z)) and the electronic energy can be represented as $E_\nu = E_\nu[\rho_0]$ (E_ν is the functional that corresponds to the ground state electron density). Therefore, the second Hohenberg-Kohn theorem can be expressed as-

$$E_\nu[\rho_t] \geq E_0[\rho_0] \tag{1.2}$$

where ρ_t corresponds to the trial electron density and $E_0[\rho_0]$ is the true ground state energy corresponding to the true electronic density ρ_0. However, it is to be noted that a trial electron density must obey the conditions $\int \rho_t(r)\mathrm{d}r = n$, where n is the total number of electrons in the molecule, and $\rho_t(r) \geq 0$ for all r. The Hohenberg-Kohn theorems were initially proved for the non-degenerate ground states. However, they have also been shown to be equally effective for degenerate ground states as well [2].

[1.2.2] The Kohn-Sham energy and the KS equations

After a year of the Hohenberg-Kohn theorem, Kohn-Sham (KS) published an approach that makes the basis of today's molecular DFT calculations [3d]. The KS approach to DFT follows a similar method to that of the Hartree-Fock approach to calculate the total energy of a molecule which in turn can be used to determine the ground state electronic properties. In order to get the total molecular energy, an initial guess of electron density is considered to obtain an initial guess of KS orbital. Thereafter, the guess KS orbitals are refined to obtain the final KS orbitals which are used to calculate the electron density and energy. The ground state electronic energy is the summation of three energy terms viz., electron kinetic energy (T), nucleus-electron attraction potential energy (V_{Ne}) and electron-electron repulsion potential energy (V_{ee}). Each of these energy terms are the functional of the ground state electron density.

$$E_0 = < T[\rho_0] > + < V_{Ne}[\rho_0] > + < V_{ee}[\rho_0] > \quad (1.3)$$

Further, the middle term in equation (1.3) i.e. the nucleus-electron attraction potential energy term can be expressed in terms of external potential ν(r) and electron density as

$$< V_{Ne}[\rho_0] > = \int \rho_0(r)\nu(\mathrm{r})dr \quad (1.4)$$

Therefore, equation (1.3) can be rewritten as

$$E_0 = < T[\rho_0] > + \int \rho_0(r)\nu(\mathrm{r})dr + < V_{ee}[\rho_0] > \quad (1.5)$$

However, equation (1.5) cannot be used directly to evaluate the ground state energy as the functional corresponds to the energy terms $< T[\rho_0] >$ and $< V_{ee}[\rho_0] >$ are not known. Therefore, in order to utilize equation (1.5), Kohn and Sham used a reference system of non-interacting electrons and introduced two new terms viz., $\Delta< T[\rho_0] >$ and $\Delta< V_{ee}[\rho_0] >$. The quantity $\Delta< T[\rho_0] >$ corresponds to the deviation of the real kinetic energy from that of the reference system ($T_r[\rho_0]$):

$$\Delta< T[\rho_0] > \equiv < T[\rho_0] > - < T_r[\rho_0] > \quad (1.6)$$

On the other hand, $\Delta< V_{ee}[\rho_0] >$ denotes the deviation of the real electron-electron repulsion energy from a classical charge-cloud coulomb repulsion energy. Mathematically, the quantity $\Delta< V_{ee}[\rho_0] >$ can be represented as:

$$\Delta< V_{ee}[\rho_0] > = < V_{ee}[\rho_0] > - \frac{1}{2}\iint \frac{\rho_0(r_1)\rho_0(r_2)}{r_{12}} dr_1 dr_2 \quad (1.7)$$

Therefore, using equations (1.6) and (1.7), the equation for the ground state energy (1.5) can be rewritten as

$$E_0 = \int \rho_0(r)\nu(r)dr + < T_r[\rho_0] > + \frac{1}{2}\iint \frac{\rho_0(r_1)\rho_0(r_2)}{r_{12}} dr_1 dr_2 \qquad (1.8)$$
$$+\Delta< T[\rho_0] > + \Delta< V_{ee}[\rho_0] >$$

The equation (1.8) again can be rewritten by introducing a new term E_{XC} which is known as the exchange-correlation energy functional or the exchange-correlation energy. The exchange-correlation energy (E_{XC}) is the sum of the kinetic energy ($\Delta< T[\rho_0] >$) and electron-electron repulsion energy ($\Delta< V_{ee}[\rho_0] >$) that were deviated from the classical system i.e. $E_{XC} = \Delta< T[\rho_0] > + \Delta< V_{ee}[\rho_0] >$

$$E_0 = \int \rho_0(r)\nu(r)dr + < T_r[\rho_0] > + \frac{1}{2}\iint \frac{\rho_0(r_1)\rho_0(r_2)}{r_{12}} dr_1 dr_2 + E_{XC}[\rho_0] \qquad (1.9)$$

Further, each term of the above expression (1.9) can be explained as follows-

(i) The first term represents the integral of the electron density with the external potential, and mathematically it can be expressed as-

$$\int \rho_0(r)\nu(r)dr = -\sum_{nuclei\ A} Z_A \int \frac{\rho_0(r_1)}{r_{1A}} dr \qquad (2.0)$$

(ii) The second term denotes reference kinetic energy for the non-interacting electron which can be expressed in terms spatial KS orbital by applying a set of Dirac and Slater-Condon rules-

$$< T_r[\rho_0] > = -\frac{1}{2}\sum_{i=1}^{2n} < \psi_i^{KS}(1)|\nabla_1^2|\psi_i^{KS}(1) > \qquad (2.1)$$

(iii) The third term of the expression (1.9) stands for classical electrostatic repulsion energy term which can be easily calculated if ρ_0 is known.

(iv) The fourth term of the equation (1.9) corresponds to the exchange-correlation energy functional which is unknown. Developing a suitable exchange-correlation functional to obtain the energy of a molecule from the electron density function is the main issue in the realm of DFT calculations.

Employing equations (2.0) and (2.1), equation (1.9) can be rewritten as

$$E_0 = -\sum_{nuclei\ A} Z_A \int \frac{\rho_0(r_1)}{r_{1A}} dr - \frac{1}{2}\sum_{i=1}^{2n} < \psi_i^{KS}(1)|\nabla_1^2|\psi_i^{KS}(1) >$$

$$+\frac{1}{2}\iint\frac{\rho_0(r_1)\rho_0(r_2)}{r_{12}}dr_1dr_2+E_{XC}[\rho_0] \tag{2.2}$$

Further, the electron density of the non-interacting reference system which is the same as that of the real ground state electron density can be expressed in terms of KS spatial orbitals-

$$\rho_0=\rho_r=\sum_{i=1}^{2n}\left|\psi_i^{KS}(1)\right|^2 \tag{2.3}$$

Combining equations (2.2) and (2.3) one can obtain the final KS equation (2.4)-

$$\left[-\frac{1}{2}\nabla_i^2-\sum_{nuclei\ A}\frac{Z_A}{r_{1A}}+\int\frac{\rho_0(r_2)}{r_{12}}dr_2+\nu_{XC}(1)\right]\psi_i^{KS}(1)=\in_i^{KS}(1)\psi_i^{KS}(1) \tag{2.4}$$

where, ν_{XC} and $\in_i^{KS}$ denotes the *exchange correlation potential* and KS energy level respectively. Further, the *exchange correlation potential* can be defined as the functional derivative of $E_{XC}[\,\rho(r)]$ with respect to $\rho(r)$ i.e. –

$$\nu_{XC}(r)=\frac{\delta\,E_{XC}[\,\rho(r)]}{\delta\rho(r)} \tag{2.5}$$

It is to be noted that the exact form of the exchange-correlation functional is not known. Therefore, in DFT calculations, a number of approximations are employed which allows the calculation of certain physical quantities quite accurately. A brief description of the DFT approximations are given below

[1.2.3] The Local Density Approximation (LDA)

The local density approximation is the simplest approximation to calculate the functional for exchange-correlation by considering a uniform electron gas model where the electron density varies very slowly with the position. By employing LDA, one can accurately determine the values of the exchange-correlation functional $E_{XC}^{LDA}[\,\rho(r)]$ (2.6) and the exchange-correlation potential ν_{XC}^{LDA} [2]. In the LDA method proposed by Slater (also known as the Xα method), the relatively small correlation part of the exchange-correlation functional is omitted and the exchange functional is used [4-6]

$$E_{XC}^{X\alpha}=E_X^{X\alpha}=-\frac{9}{8}\left(\frac{3}{\pi}\right)\alpha\int[\,\rho(r)]^{\frac{4}{3}}dr \tag{2.6}$$

[1.2.4] The Local Spin Density Approximation (LSDA)

It is the extension of LDA, where reasonably better results are obtained compared to that of LDA by considering the spin of the electrons of the uniform gas model. This approximation is highly useful for systems featuring one or more unpaired electrons. However, for systems possessing all paired electrons, LSDA is equivalent to LDA. The local spin density approximation gives quite good results for geometry optimization, frequencies and electron distribution properties but performs poorly in dissociation energy calculation.

[1.2.5] The Generalized-Gradient Approximation (GGA)

The LDA/LSDA which considers a uniform gas model is not applicable to real systems where the electron density varies greatly from one place to another. Therefore, DFT calculations that are performed employing these approximations might have serious issues. However, it is to be noted that most of the functional that are employed nowadays for DFT calculations not only use the LSDA but also use the electron density and its gradient. These types of functional are commonly known as gradient corrected functional. In general, more accurate results for molecular geometry and ground state energy can be obtained by employing the GGA functional. LYP [7], B88 [8] and PW91 [9] are some examples of GGA functional. Mathematically the GGA exchange correlation energy functional can be expressed as-

$$E_{XC}^{GGA} = \int \rho(r)\varepsilon_{XC}[\rho(r), |\nabla\rho(r)|]dr \tag{2.7}$$

Further, the updated version of the GGA functionals is the meta-GGA functional in which the exchange-correlation energy functional (E_{XC}^{mGGA}) considers not only the local electron density ($\rho(r)$) and its derivatives ($\nabla\rho(r)$) but also the second derivative or the laplacian of the electron density ($\nabla^2\rho(r)$) and the local kinetic energy density (τ). TPSS [10], KCIS [11] and M06–L [12] etc. are some examples of mGGA functional. The exchange correlation functional for mGGA can be written as-

$$E_{XC}^{mGGA} = \int \rho(r)\varepsilon_{XC}[\rho(r), |\nabla\rho(r)|, \nabla^2\rho(r)\tau]dr \tag{2.8}$$

where τ represents the local kinetic energy density that can be expressed as-

$$\tau = \frac{1}{2}\sum_i |\nabla\psi_i(\mathrm{r})|^2 \tag{2.9}$$

[1.2.6] Hybrid Functional

Nowadays, hybrid functionals are widely used in different DFT calculations. The exchange-correlation part of the hybrid functionals contain an exact exchange energy term which is obtained from Hartree-Fock theory. Mathematically, the exact exchange energy (E_X^{HF}) term can be expressed as-

$$E_X^{HF} = -\sum_{i=1}^{n}\sum_{j=1}^{n} < \psi_i^{KS}(1)\psi_j^{KS}(2)\left|\frac{1}{r_{ij}}\right|\psi_i^{KS}(2)\psi_j^{KS}(1) > \qquad (3.0)$$

The E_X^{HF} term corresponds to the exact exchange energy for a system containing non-interacting electrons. B3LYP [13] and PBE0 [14] are some commonly used examples of hybrid functional.

[1.3] Basis Set

A basis set is a set of functions (also known as basis functions) that are employed to obtain molecular orbitals. In quantum chemical calculations, the basis functions are composed of atomic orbital of atoms which are combined linearly to achieve the molecular orbitals. Two types of atomic orbitals that are commonly used in computational chemistry viz., Gaussian-type orbital [15] and Slater-type orbital [16], and can be expressed by the following equations (3.1) and (3.2) respectively for 1s orbital.

$$\varphi_{ST} = \mathrm{N}e^{(-\alpha r)} \qquad (3.1)$$

$$\varphi_{GT} = \mathrm{N}e^{(-\alpha r^2)} \qquad (3.2)$$

The basic difference between these two sets of atomic orbitals is that the Gaussian type orbital involves the square of the radius (r^2) (3.2) whereas the Slater type of orbitals involve only r (3.1). Furthermore, it should be noted that compared to the GTOs, the STOs are more accurate. However, the two electron integral over the STOs is difficult to calculate compared to that of the GTOs. Therefore, in order to solve this issue, a linear combination of sufficient GTOs are employed to mimic the STOs.

The basis sets can be divided into two broad groups viz., minimal basis set and extended basis set. The minimal basis sets are the simplest ones and can be expressed as STO-nG, where n signifies the number of GTOs that are used to represent each STOs. STO-3G, STO-4G and STO-6G are some common examples of minimal basis sets [17]. Generally, minimal basis sets are much cheaper (required less time) but they give results that are not accurate or reliable to study different electronic properties of substances. On

the other hand, the extended basis sets define the atomic orbitals more accurately and hence, the results obtained by using them are quite reliable. A brief explanation of the different extended basis sets is given below-

The split valence basis sets provide a better description of the valence electrons where the valence orbitals are divided into two or more basis functions. 3-21G [18] is an example of a split valence basis set where the non-valence electrons are defined by a single basis function consisting of three Gaussian functions. On the other hand, the valence orbitals are described with two types of basis functions where the first one is comprised of two Gaussian functions while the second one is composed of only one Gaussian function. 4-31G [19], 6-31G [20] and 6-311G [21] are some commonly used examples of split valence basis sets.

In case of real molecules, when the atoms approach each other, they generally undergo polarization. Therefore, in order to increase the flexibility of the orbital description, polarization functions are used. Two different notations are used to specify the addition of polarization to the basis set. The first notation employs the addition of an asterisk (*) to indicate the addition of polarization function to the non-hydrogen atoms whereas two asterisks (**) denote the addition of polarization function to all atoms including hydrogen. The second one employs higher angular quantum numbers to signify the addition of polarization to the basis functions. For example, the basis functions 6-311G* and 6-311G** can also be denoted as 6-311G(d) and 6-311G(d,p) respectively.

On the other hand, for anionic systems or molecules having lone pairs, diffuse functions are used that can effectively describe different electronic properties of systems possessing diffuse charge distribution. An addition of the '+' sign to the standard notation of the basis set, indicate the addition of diffuse basis functions on all atoms (except hydrogen) whereas a '++' sign reflects the addition of diffuse functions not only to the heavy atoms but also to the lighter hydrogen atoms. 6-31+g*, 6-31+G** and 6-311++g* are some commonly used examples of diffuse basis sets that are employed to study different electronic properties of systems featuring diffuse electron clouds.

[1.3.1] Effective Core Potential (ECP)

The effective core potential is generally useful for the system that features heavier transition metals (TM). As the heavier TMs contain a large number of core electrons,

therefore, molecules bearing TM are computationally more demanding in nature. However, this problem can be solved (without compromising the accuracy of the results) by employing effective core potentials which replace the core electrons with an effective potential [22]. In addition to saving time, ECP also effectively takes care of the relativistic effect which is strongly governed by the core electrons of the heavier TMs. Mathematically, the effective core potential can be expressed as-

$$ECP(r) = \sum_{i=1}^{k} c_i \, r^{n_i} e^{-\alpha_i r^2} \qquad (3.3)$$

LANL2DZ [23] and SDD [24] are some popularly used basis sets for TMs which employ ECP for the core electrons.

Furthermore, to calculate the molecular structure and chemical activities of systems with heavier TM atoms, it is crucial to consider the relativistic effect. In order to incorporate the relativistic effect in theoretical calculations, the Dirac equation is typically used instead the nonrelativistic Schrödinger equation. However, the Dirac equation is valid only for one electron system. Therefore, it is necessary to extend the one-electron Dirac Hamiltonian to a many-electron Hamiltonian so that it can be applied for systems with many electrons. This is generally done by combining the one-electron Dirac Hamiltonian with Coulomb or Breit operator. However, the four component relativistic approach is computationally demanding and difficult to use for larger systems. Therefore, a number of two-component quasi-relativistic approaches have been proposed that are effective for chemical systems with heavier TM centers. One such popularly used approach is Douglas-Kroll-Hess (DKH) approach which decouples the small and large components of the Dirac spinors in the presence of an external potential by performing several unitary transformation. This DKH approach [25] has been widely used to determine molecular geometry, frequencies and electron affinities etc., [26].

[1.4] Quantum Theory of Atoms in Molecules (QTAIM)

Bader's quantum theory of atoms in molecules (QTAIM) is popularly used to obtain a comprehensive understanding of the bonding situation in molecules in terms of electron density ρ(r). In QTAIM, an atom of a molecule is considered as a region of real space that is bounded by a surface $S(r_S)$ of local zero flux in the gradient vector field of the electron density ρ(r) [27]. Mathematically it can be expressed as follows-

$$\nabla\rho(r).n(r) = 0 \quad \forall\, r \in S(r_S) \qquad (3.4)$$

A brief description of some of the commonly used terminology in QTAIM are given below-

Bond Path: A bond path represents a single line of maximum electron density via which the nuclei of the chemically bonded atoms are connected in a molecule.

Bond Critical Point (BCP): Again, in a bond path, there reside a certain point known as bond critical point (BCP) where the first derivative of the electron density vanishes i.e. $\nabla\rho(r) = 0$. Further, it should be noted that the electron density at the BCP can be used as an effective measure to evaluate the nature of the chemical bonds. Usually, a covalent (also referred to as shared or open-shell) type of interaction is characterized by a large value of ρ_b (> 0.2 a.u.) and large and negative values of $[\nabla^2\rho(r)]$. In contrast, for closed-shell interactions (e.g., van der Waals, ionic or hydrogen bond interaction), ρ_b is small (< 0.1 a.u.) while its laplacian $[\nabla^2\rho(r)]$ is positive.

Further, depending upon the number of negative eigenvalues of the Hessian matrix of real space function, the critical points (CPs) can be classified into three categories [28]-

(3,-3): This class of CP is known as nuclear critical point (NCP) where all three eigenvalues of the Hessian matrix of function are negative. For electron density analysis, the NCP appears at the nuclear positions.

(3,+1): In this case, only one eigenvalue of the Hessian matrix of function is negative and this class of CP is known as ring critical point (RCP) and for electron density analysis, it appears at the center of a ring.

(3,+3): In this class of CP, all the eigenvalues of the Hessian matrix of function are positive and is known as cage critical point (CCP). For electron density analysis the CCP generally appears in the center of a cage system.

[1.5] Energy Decomposition Analysis (EDA)

Energy decomposition analysis can be considered as a powerful tool to obtain a quantitative understanding of chemical bonds [29, 30]. EDA focuses on the instantaneous interaction energy (ΔE_{int}) associated with the interaction between two fragments in a molecule which can be divided into four components: $\Delta E_{int} = \Delta E_{elstat} + \Delta E_{Pauli} + \Delta E_{orb} + \Delta E_{disp}$. The ΔE_{elstat} term represents the electrostatic interaction energy between the fragments. ΔE_{Pauli} corresponds to the repulsive interactions between the fragments which are caused by the destabilizing interactions between occupied orbitals of both the fragments while ΔE_{orb} and ΔE_{disp} refer to the stabilizing orbital and dispersion interactions

respectively. Again, the ΔE_{orb} term further can be decomposed into the contribution of orbital with different symmetry.

Let us consider fragments A° and B° with corresponding wave functions Ψ_A^0 and Ψ_B^0 and energies E_A^0 and E_B^0 that combine to give molecule A–B with wave function Ψ_{AB} and energy E_{AB}. During the formation of A–B, the fragments A^0 and B^0 undergo distortion from their ground state geometries. In addition, their corresponding wave function Ψ_A^0 and Ψ_B^0 also changes to the electronic state Ψ_A and Ψ_B with energies E_A and E_B respectively. The energy that is required to distort and electronically change the fragments A^0 and B^0 to form the molecule A–B is known as preparation energy ΔE_{prep} (3.5).

$$\Delta E_{prep} = E_A - E_A^0 - E_B - E_B^0 \tag{3.5}$$

Again the interaction energy ΔE_{int} can be defined as the difference in the energy of the molecule A–B (E_{AB}) and the energies of the prepared fragments A (E_A) and B (E_B) (3.6).

$$\Delta E_{int} = E_{AB} - E_A - E_B \tag{3.6}$$

The sum of the interaction energy (ΔE_{int}) and the preparation energy (ΔE_{prep}) corresponds to the bond dissociation energy (D_e) i.e. – $D_e = \Delta E_{int} + \Delta E_{prep}$.

In the first step of the EDA calculation, the distorted fragments A and B with frozen charge densities are brought from infinite separation to the required position in the molecule. In this state, the wavefunction of the premolecule is the product of the wavefunction of A and B i.e. $\Psi_A\Psi_B$ with energy E_{AB}^0. The Coulomb interaction between the frozen charge densities of A and B at the equilibrium geometry of the molecule A–B (ΔE_{elstat}) can be mathematically expressed by the equation (3.7). The ΔE_{elstat} interaction in most cases is attractive.

$$\Delta E_{elstat} = \sum_{\alpha \epsilon A}\sum_{\beta \epsilon B}\frac{Z_\alpha Z_\beta}{R_{\alpha\beta}} + \int dr\, V_B(r)\rho_A(r) + \int dr\, V_A(r)\rho_B(r) + \iint dr_1 dr_2 \frac{\rho_A(r_1)\,\rho_B(r_2)}{r_{12}} \tag{3.7}$$

In the second step of the EDA calculation, the product of the $\Psi_A\Psi_B$ is renormalized (as $\Psi_A\Psi_B$ violates the Pauli principle) to give an intermediate state Ψ^0 with energy E^0. The energy difference between the E^0 and E_{AB}^0 is known as exchange (Pauli) repulsion (ΔE_{Pauli}) i.e. $\Delta E_{Pauli} = E_{AB}^0 - E^0$

The third step involves the generation of the final state wavefunction Ψ_{AB} with energy E_{AB} from the intermediate state Ψ^0. This step involves the lowering of the energy

of the molecule A–B that comes from the orbital mixing of the fragments A and B which is termed as orbital interaction (ΔE_{orb}) i.e. $\Delta E_{orb} = E_{AB} - E_{AB}^{0}$. The ΔE_{orb} term can be decomposed into the contribution of orbital with different symmetry which can be mathematically expressed as

$$\Delta E_{orb} = \sum_{\Gamma} \Delta E_{\Gamma} \tag{3.8}$$

Where Γ represents the reducible representation of the point group of the molecule. Furthermore, the energy associated with the dispersion effects are also calculated in the EDA calculations (ΔE_{disp}).

[1.6] Activation Strain Model (ASM)

The activation strain model (ASM) [31] also known as the *distortion*/*interaction* model [32] helps us to obtain a deeper understanding of different physical factors which governs the activation barrier involved in different chemical reactions [33]. ASM is a fragment approach in which the barrier height involved in a chemical reaction is described in terms of initial reactants. Within the ASM method, the potential energy surface $\Delta E(\zeta)$ is decomposed along the reaction coordinate, ζ, into two contributions, namely the strain $\Delta E_{strain}(\zeta)$ associated with the deformation (or distortion) required by the individual reactants during the process and the interaction $\Delta E_{int}(\zeta)$ between these increasingly deformed reactants:

$$\Delta E(\zeta) = \Delta E_{strain}(\zeta) + \Delta E_{int}(\zeta)$$

The strain $\Delta E_{strain}(\zeta)$ represents the rigidity of the reactants and the extent of reorganization that a group must undergo during the reaction. Generally, the $\Delta E_{strain}(\zeta)$ values are positive i.e. destabilizing in nature. On the other hand, the interaction $\Delta E_{int}(\zeta)$ between the reactants are strongly governed by their electronic structure and their orientation when they approach each other. Mostly, the term $\Delta E_{int}(\zeta)$ is negative i.e. stabilizing in nature.

[1.7] A brief description of the remaining chapters

[1.7.1] Chapter 2: In Search of Stable, Singlet Metalla *N*-Heterocyclic Carbene (MNHC) and Probing their Potential in Small Molecule Activation.

The chemistry of carbenes has evolved as an important area of research over the last couple of decades because of their ease of tunability and versatile catalytic applicability [34–36]. Even though the parent carbene ($:CH_2$) prefers to have a triplet ground state [37, 38], a thorough search of the literature yields a large number of carbenes which favor the singlet state over the triplet state. A signature example of this class of carbene is *N*-heterocyclic carbene (NHC), which was synthesized and isolated by Arduengo et al. in 1991 [39].

This chapter is divided into parts- (i) the first part deals with the computational study aimed towards designing a series of stable, singlet MNHCs, and (ii) in the second part, we have probed the potential of the MNHCs towards activation of a variety of enthalpically strong E–H bonds (E = H, N, P, Si and C).

[1.7.1.1] In Search of Stable Singlet Metalla-*N*-Heterocyclic Carbenes (MNHCs): A Contribution from Theory

Many transition metal (TM) complexes have been synthesized bearing NHC as a ligand [40–47] and some of these complexes are being successfully employed in homogeneous catalysis [35,36]. The electron donation ability of the carbene ligand plays a crucial role in determining the catalytic efficiency of the corresponding TM complexes. Therefore, a lot of emphasis has been put towards the design and synthesis of carbenes with better ligand properties and this was generally accomplished by changing either the heteroatom attached to the carbene center or by changing the substituents at the heteroatom as well as by modifying the ring framework itself. For example, the amino group of the carbene ring framework was substituted by other heteroatoms such as phosphorus (PHC) [48,49], oxygen (oxazol-2-ylidene) [50] and sulphur (thiazol-2-ylidene) [50–53]. Other strategies include the alteration of the carbene carbon position (a mesoionic or abnormal carbene) [54–57], considering a saturated backbone instead of an olefinic backbone [58], expansion of the ring size [59–62], etc. Similarly, attempts have been made to incorporate transition metal (TM) fragments into the carbene ring framework by replacing one of the backbone carbon fragments by isolobal metal fragments [63,64]. These types of NHCs

containing TM fragments within the carbene ring framework are commonly known as metalla-*N*-heterocyclic carbenes (MNHCs). Interestingly, the computed proton affinity and the pK_a values for the MNHCs are found to be significantly higher than those of traditional NHCs [65], indicating their higher degree of σ-donation ability. Even though MNHCs exhibit better electron donation ability than NHCs, their isolation in the free crystalline state remains an experimental challenge [64]. However, they can be trapped by forming adducts with transition metal complexes such as [AuCl(PPh_3)], [Rh(cod)Cl_2] and CuCl [65].

In this part, we have performed density functional theory calculations to design a series of stable, singlet MNHCs (Scheme 1.1). We have used hybrid PBE0 exchange–correlation functional [66,67] in conjunction with the 6-311++G** [68–70] basis set for the main group elements as well as for the first-row transition metals. Furthermore, the relativistic all electron QZP-DKH [71] basis set was considered for heavier transition metal ruthenium with the relativistic second order DKH(DKH2) Hamiltonian [72]. All the MNHCs considered in this study are found to exhibit a stable singlet ground state. The introduction of π-donor groups such as OMe and NMe_2 at the carbene framework significantly increases the ΔE_{S-T} values for the five-membered MNHCs. Furthermore, the

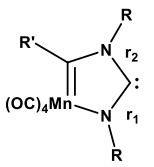

1; R=CH_3, R' = H (**1a**)
R' = NMe_2 (**1b**)
R' = OMe (**1c**)

1'; R =Ph, R' = H (**1'a**)
R' = NMe_2 (**1'b**)
R' = OMe (**1'c**)

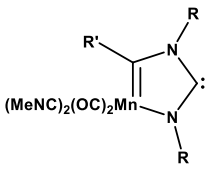

2; R=CH_3, R' = H (**2a**)
R' = NMe_2 (**2b**)
R' = OMe (**2c**)

2'; R =Ph, R' = H (**2'a**)
R' = NMe_2 (**2'b**)
R' = OMe (**2'c**)

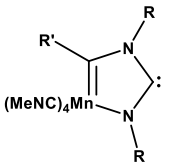

3; R=CH_3,R' = H (**3a**)
R' = NMe_2 (**3b**)
R' = OMe (**3c**)

3'; R =Ph, R' = H (**3'a**)
R' = NMe_2 (**3'b**)
R' = OMe (**3'c**)

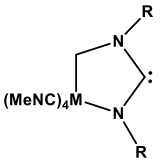

4; R = CH_3, M =Fe (**4a**)
M = Ru (**4b**)

4'; R = Ph, M =Fe (**4'a**)
M =Ru (**4'b**)

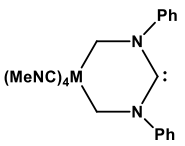

5a, M = Fe
5b, M = Ru

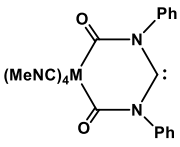

6a, M = Fe
6b, M = Ru

Scheme 1.1: Schematic representation of the range of MNHCs considered in this study.

calculated ΔE_{S-T} values for some of the MNHCs are found to be significantly large (30–50 kcal mol^{-1}) and lie within the range of the experimentally known carbenes. Therefore, these computationally designed MNHCs – especially those with the ΔE_{S-T} values of more than 40.0 kcal mol^{-1} may be considered to be ideal candidates for experimental realization.

[1.7.1.2] Probing the Potential of Metalla-*N*-Heterocyclic Carbenes Towards Activation of Enthalpically Strong Bonds

In this part, we have performed in-depth computational studies aimed towards probing the efficiency of the MNHCs in activation of small molecules (Scheme 1.2). We have used meta-GGA M06 [73] exchange–correlation functional in conjunction with the valence polarized def2-TZVP basis set for all the elements [74,75]. All the MNHCs have been found to have a stable singlet ground state and exhibit superior electron donating and accepting ability compared to their respective parent carbenes. Furthermore, the calculated energy barrier for the activation of a variety of enthalpically strong bonds for the MNHCs, **1** and **3** are found to be comparable to those obtained for the experimentally evaluated carbenes cyclic(alkyl)(amino)carbene (CAAC) and diamido carbene (DAC), indicating their potential in small molecule activation.

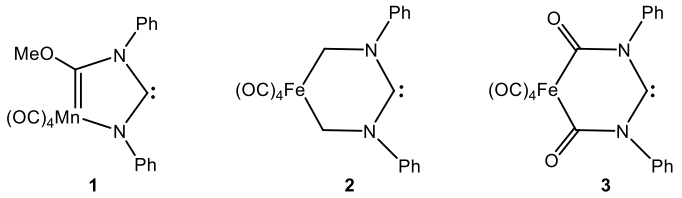

Scheme 1.2: Schematic representation of the MNHCs considered in this study.

[1.7.2] Chapter 3: Activation of Small Molecules by Cyclic Alkyl Amino Silylenes (CAASis) and Germylenes (CAAGes): A Theoretical Study

The chemistry of silylenes and germylenes are fairly diverse both in structure and reactivity. *N*-heterocyclic silylene (NHSi) [76] (Scheme 3.1) and germylene (NHGe) [77] are neutral divalent species with a vacant p–orbital and a non–bonding pair of electrons. A majority of the silylenes and germylenes possess a singlet ground state which may be attributed to the increased radial extension of ns and np orbitals as we go down the group [78]. The ligating properties of NHEs (E = Si, Ge) are somewhat different from their lighter congeners as NHCs possess a higher Lewis basicity and lower Lewis acidity than NHSis/NHGes [79]. Recently, the research groups of Iwamoto [80] and Kinjo [81]

independently reported the isolation of silicon (CAASi) and germanium (CAAGe) analogs of cyclic(alkyl)(amino)carbene (CAAC) [82] where the central silicon or germanium atom is bonded to a nitrogen and a quaternary carbon atom. These cyclic(alkyl)(amino)silylenes (CAASi) and cyclic(alkyl)(amino)germylenes (CAAGe) are found to have better electron donation ability than classical NHSis and NHGes. Very recently, Iwamoto and co-workers found that CAASi could be used as a dehydrogenation reagent [83]. However, compared to the large number of studies available on CAACs, to the best of our knowledge, there exists no systematic and comprehensive study–either experimental or computational, on CAASis and CAAGes.

In this part, we present our results of computational studies on the electronic and ligand properties of skeletally substituted CAASis and CAAGes, and based on their ligand properties, some of these molecules are probed towards activation of small molecules (Scheme 1.3). We have employed meta-GGA M06 [73] exchange correlational functional in conjunction with def2-TZVP basis set for all the atoms [74,75]. All the skeletally substituted cyclic alkyl amino silylenes (CAASis) and germylenes (CAAGes) considered in this study compute significantly higher or comparable singlet-triplet separation ($\Delta E_{S\text{-}T}$) than their synthetically accessible parent analogues implying that all of them may be stable

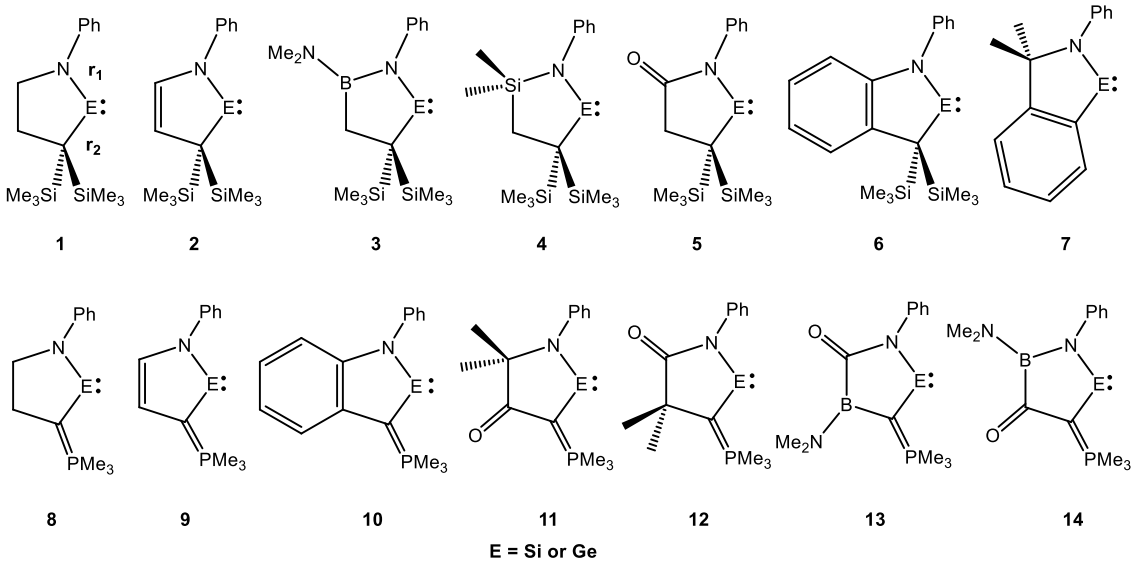

Scheme 1.3: Schematic representation of the range of silylenes and germylenes considered in the present study.

enough for experimental realization. Furthermore, some of the computationally designed CAASis and CAAGes are probed towards activation of H–H, N–H, C–H and Si–H bonds and the energetics of these reactions are compared with those of the experimentally

evaluated systems including Driess's NacNac stabilized silylene and Kira's five-membered silylene. Our study successfully explains many of the experimental observations, e.g., requirement of higher temperature for C–H and Si–H bond activations.

[1.7.3] Chapter 4: **Ylide Decorated Monovalent Group 13 Carbenoids and Probing their potential towards Activation of Enthalpically Strong Bonds**.

This chapter is divided into two parts-(i) the first part deals with the stabilization of the hitherto unknown five-membered cyclic boron(I) carbenoids and studying their potential in small molecule activation. (ii) In the second part, we have proposed a couple of ylide decorated monovalent aluminium and gallium carbenoids with enhanced ligand properties and studied their reactivity towards activation of a variety of entalpically strong bonds.

[1.7.3.1] Stable *N*-Heterocyclic Borylenes with Promising Ligand Properties: A Contribution from Theory

The monovalent group 13 carbenoids which are isoelectronic to the divalent group 14 compounds (e.g. NHC), are known for the heavier Al–Tl(III) [84–87] derivatives and are found to be capable of exhibiting metallomimetic behaviour such as small molecule activation [88]. The first addition to this class of compounds came from Roesky and coworkers with the isolation of a neutral six membered Al(I) carbenoid supported by a bulky β-diketiminate (NacNac) ligand framework [84]. This was followed by the synthesis of its gallium analogue by Power and coworkers [85]. However, the synthesis and isolation of a neutral monomeric cyclic boron(I) carbenoid has remained elusive to date; which may be attributed to smaller energetic separation between the valence s and p orbitals as well as low singlet–triplet (ΔE_{S-T}) separation [89,90]. Phosphorous ylides are found to be useful in stabilizing group 14 bases [91–97]. By virtue of the presence of a pseudo lone pair at the carbon atom, these ylides can function as strong π-donating substituents that can be employed towards the stabilization of reactive low-valent main-group species [98]. Based on these reports, we envisage that phosphorous ylides could be promising systems for the stabilization and isolation of the hitherto unknown cyclic boron(I) carbenoids.

In this part, we present the results of our computational studies on the stabilization of neutral, monomeric five-membered boron(I) carbenoids by employing two different ylide functionalities, viz., a conventional carbon-based phosphorous ylide and a

zwitterionic four-membered cyclic ylide (Scheme 1.4) and their potential in small molecule activation. We have used meta-GGA M06 exchange–correlation functional [73] in combination with the valence polarized def2-TZVP basis set for all the elements [74, 75]. Calculations suggest that strongly π-electron donating groups such as amino or

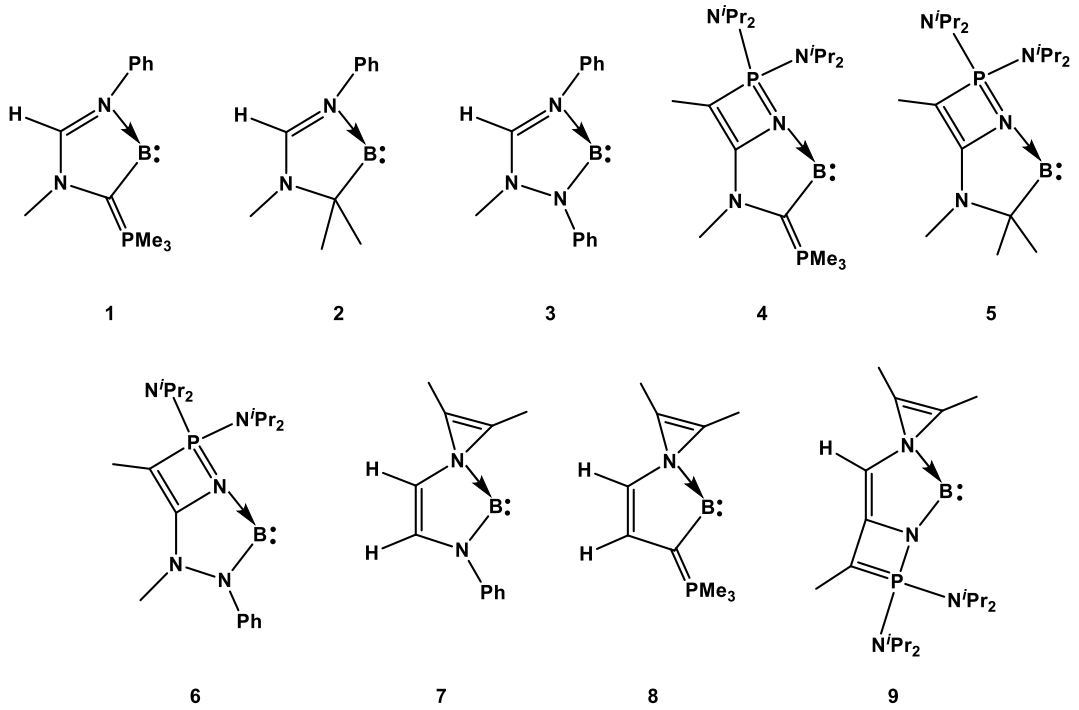

Scheme 1.4: Schematic representation of the cyclic five-membered boron(I) carbenoids considered in this study.

ylides may be used for the stabilization of neutral monomeric five-membered boron(I) carbenoids (**1**–**9**, Scheme 1.4). It is encouraging to note that the molecules **4**–**7** and **9** compute the highest singlet-triplet separation values ($\Delta E_{S\text{-}T}$ = 25.5–42.3 kcal mol^{-1}) known to date, and to the best of our knowledge, no other cyclic borylenes are known with such large values thus highlighting the remarkable power of ylides in stabilizing unusual species. In addition, the calculated $\Delta E_{S\text{-}T}$ values are found to be either comparable or higher than that of the synthetically amenable Roesky's Al(I) carbenoid (34.1 kcal mol^{-1}) or cAAC (42.7 kcal mol^{-1}) further providing a hint towards their possible isolation. In addition, **4**–**7** and **9** are remarkably nucleophilic and compute considerably lower barrier heights for the activation of E–H (E = H, C and N) and C–F bonds compared to that of the experimentally evaluated systems indicating their potential in small molecule activation.

[1.7.3.2] Unravelling the Potential of Ylides in Stabilizing Low-Valent Group 13 Compounds: Theoretical Predictions of Stable, Five-membered Group 13 (Al and Ga) Carbenoids Capable of Small Molecule Activation

Motivated by the lack of isolable neutral monomeric five-membered aluminium carbenoids as well as to contribute to the field of group 13 carbenoids with enhanced ligand properties, density functional theory calculations were carried out on a number of ylide decorated monovalent aluminium and gallium carbenoids (**1**–**4**, Scheme 1.5). We have employed meta-GGA M06 exchange–correlation functional [73] in combination with the valence polarized def2-TZVP basis set for all the elements [74,75]. All the

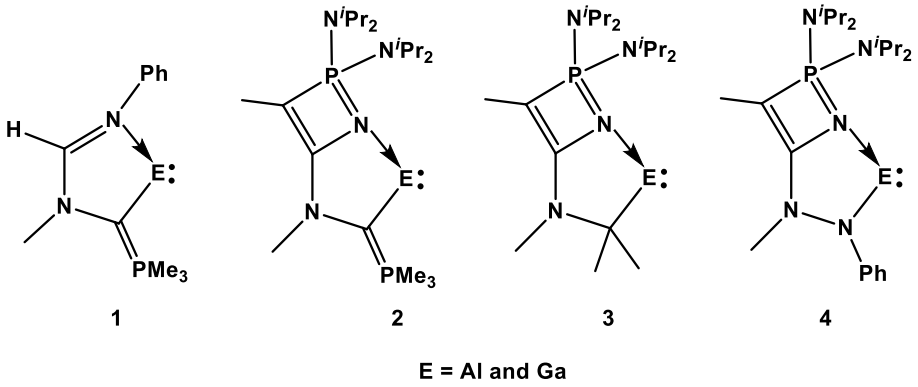

Scheme 1.5: Schematic representation of the group 13 carbenoids considered in this study.

computationally proposed molecules (**1**-**4**) are found to be substantially nucleophilic and exhibit singlet-triplet energy separation values that are either comparable or higher than those obtained for **I**, **II** and **XIa** indicating that all of them could be considered as potential synthetic targets. In addition, the calculated activation energy barriers obtained for **1**–**4** in different bond activation processes are found to be comparable to those of **I** and **II** which are known to activate a range of small molecules under mild reaction conditions. Therefore, akin to **I** and **II**, all the newly designed ylide anchored group 13 carbenoids may be considered as suitable candidates for small molecule activation and calls for sustained experimental efforts toward their synthesis and isolation.

[1.7.4] Chapter 5: **Understanding, Modulating and Leveraging Transannular M→Z Interactions**

Transition metal complexes with group 13 elements have attracted considerable interest over the last few decades because of their atypical donor–acceptor interactions in which the transition metal and the ligand play inverted roles [99, 100]. Due to the availability of

a vacant p orbital, trivalent compounds of group 13 elements can act as σ-acceptor ligands. Transition metal complexes containing group 13 element as a σ-acceptor group are commonly known as group 13 metallatranes and feature a transannular M→Z interaction. It is believed that this interaction plays a key role in governing the stability and reactivity of these molecules. Group 13 metallatranes are found to be useful in various catalytic processes, such as dinitrogen activation [101–103], hydrogenation and hydrosilylation of CO_2 [104,105], catalytic olefin hydrogenation [106] and heterolytic E–H bond activation (E = O, S, C, N) [107–111] etc. The flexibility of the M→Z interaction is believed to play a key role in dictating the catalytic activities of group 13 metallatranes.

In this work, we perform a comprehensive, in-depth analysis of the nature and strength of the intramolecular transannular interaction present in these molecules aiming at providing valuable information for their use in catalysis and small molecule activation reactions. The transannular M→Z interaction is analyzed as a function of different equatorial (E), apical (L), and Lewis acidic (Z) groups (Scheme 1.6). We have used meta

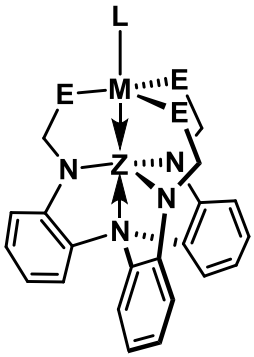

E= S^{i}Pr, P(^{i}Pr)$_2$; M= Fe, Co, Ni; Z= Al, Ga, In

L= NH_3, PMe_3, N_2, CO, NHC, aNHC, CNMe

Scheme 1.6: Schematic representation of the metallatranes considered in this study.

hybrid exchange-correlation energy functional M06 [73] in conjunction with the split valence polarized def2-SVP basis set [74, 75] for H, C, N, O, S, and P, and the triple-zeta valence polarized def2-TZVP basis set [74, 75] for Fe, Co, Ni, Al, Ga, and In. The core electrons of In were replaced by an effective core potential (ECP). The extent of these transannular M····Z interactions depends to a large extent on the size and polarizability of the group 13 element (Z group). Furthermore, it should be noted that the strength of the transannular interaction plays a decisive role in governing the reactivity of the TM center in metallatranes. For example, the calculated reaction free energies (ΔG°) for binding of

different Lewis bases are found to be more exergonic for the larger, more polarizable Lewis acidic In(III) ion than those for Al(III) or Ga(III) ions [112]. Therefore, such transannular interactions could be leveraged towards the binding of σ-donor or π acidic ligands to a given transition metal center. The quantum theory of atoms in molecules study also suggests the presence of considerable electron density (ρ) at the BCP of the M····Z bonds, which gradually increases as Z is varied down group 13 from Al to Ga to In. In addition, the calculated local electronic energy density (H(r)) values are found to be negative, indicating the covalent nature of the M····Z bonds. Furthermore, EDA-NOCV analysis indicates the strong binding ability of these metallatranes not only to different σ-donor and π acceptor ligands but also to relatively inert species, such as N_2.

[1.7.5] Chapter 6: Unravelling the Potential of Tripodal Vanadium Complexes toward Dinitrogen Reduction

The element nitrogen is highly essential for life on earth. Although, dinitrogen is one of the most available molecules surrounding us, due to its high thermodynamic stability (945 kJ mol^{-1}) [113] and nonpolar nature, it is one of the most inert gas that can be used for chemical processes. The best method known till date for the reduction of dinitrogen to ammonia is the Haber-Bosch process which demands a very high degree of temperature (400–500 °C) and pressure (~200 atm) [114, 115]. Interestingly, the same process is performed by nature at ambient conditions with the assistance of certain group of enzyme known as nitrogenase which contain transition metal (TM) such as Fe (iron-only nitrogenase), Mo (molybdenum nitrogenase) and V (vanadium nitrogenase) in their active site [116]. The enzyme nitrogenase contains two protein units. The larger one is called Fe-Mo protein consisting of two P-clusters that helps in electron transfer process while the other unit contain two iron molybdenum cofactor (FeMocos) where reduction of dinitrogen takes place [117, 118]. Therefore, efforts are being made to mimic the active site of nitrogenase enzyme by developing suitable TM based model systems that can carry out the reduction process under ambient conditions [119-122].

In 2003, Schrock and coworkers synthesized the first nitrogenase model system that can catalytically convert dinitrogen into ammonia [123]. They have used a molybdenum complex with sterically encumbered $HIPTN_3N$ ligand ({$HIPTN_3N$ = [{3,5-(2,4,6-$^{i}Pr_3C_6H_2$)$^{2-}$ $C_6H_3NCH_2CH_2$}$_3$N]$^{3-}$}) by the use of lutidinium [Lut] as a proton source and decamethylchromocene as a reductant and the overall yield was found to be

66%. In order to understand the mechanistic details of the N_2 reduction process, several intermediates were isolated and DFT calculations were performed [124-127]. A few years later, in 2011, Nishibayashi and coworkers developed a dinuclear molybdenum dinitrogen complex supported by PNP pincer ligand which can produce up to 11.6 equivalent of NH_3 per molybdenum center by employing cobaltocene as reductant and lutidinium triflate as proton source [128]. Furthermore, in 2017, they have developed another interesting dinuclear molybdenum system with *N*-heterocyclic carbene (NHC)-based PCP-pincer ligands which shows remarkable catalytic activity towards the reduction of dinitrogen to ammonia (230 equiv. of NH_3), the most effective catalyst synthesized to date [129]. Over the years, Peters and coworkers have synthesized and characterized a number of iron based model systems that can mimic the biological activity of nitrogenase enzyme. Most of the dinitrogen model systems that have been designed to date mostly contain iron and molybdenum at their active site. However, a few of model systems with different transition metal (other than iron and molybdenum) have also been reported [130]. For example, Lu and coworkers have synthesized a dicobalt complex which could mediate the catalytic conversion of dinitrogen to silylamines under suitable conditions [131]. More recently, Peters and coworkers successfully synthesized tris(phosphine)sily ligand supported osmium and ruthenium complexes which are capable of furnishing ammonia from dinitrogen under ambient pressure and low temperature [132]. Furthermore, it should be noted that in terms of efficiency, the vanadium nitrogenase stands next to the molybdenum nitrogenase, however, only a few number of synthetic vanadium based complexes are known which can catalytically facilitate the conversion of dinitrogen to ammonia [133]. Therefore, there is a need to design and study a variety of biomimetic vanadium based systems which can carry out the dinitrogen reduction process.

In this work we have performed in depth comprehensive study aimed towards designing of a series of tripodal vanadium complexes (Scheme 1.7) and studied their efficiency in some of the key steps involved in the dinitrogen reduction process. We have used M06-L functional [134] in conjunction with 6-311+g* basis set [68–70] for all the elements. All our proposed complexes are found to be capable of dinitrogen functionalization as reflected in the thermodynamic feasibility of several key steps (binding of nitrogen, formation of the diazenido and nitride complex etc.) investigated in this study. In addition, we have performed a comprehensive mechanistic study to

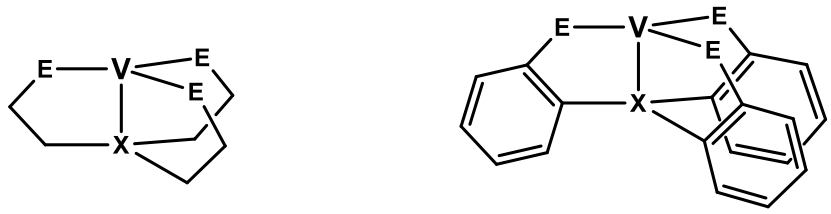

E = P^{i}Pr$_2$, X = C (1a')
X = Si (1b')
X = B (1c')
E = S^{i}Pr, X = C (1d')
X = Si (1e')
X = B (1f')

E = P^{i}Pr$_2$, X = C (1a")
X = Si (1b")
X = B (1c")
E = S^{i}Pr, X = C (1d")
X = Si (1e")
X = B (1f")

Scheme 1.7: Schematic representation of the model vanadium complexes considered in this study.

understand the efficiency of the catalysts **[1c′′]** and **[1f′′]** towards dinitrogen reduction process by considering all possible pathways viz., alternating and distal pathways (Scheme 1.8). Both thermodynamic and kinetic studies reveal the viability of these two pathways.

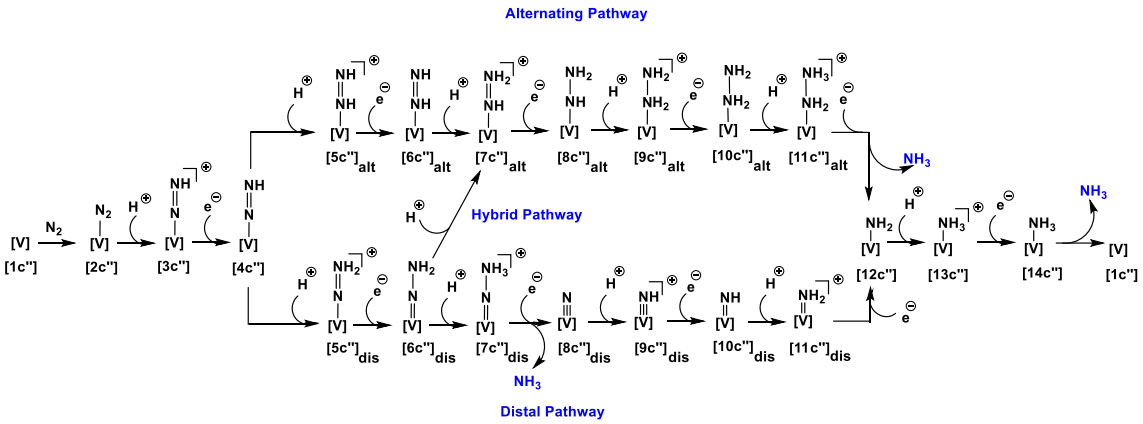

Scheme 1.8: Alternating, hybrid and distal pathways for dinitrogen reduction to NH_3.

Our calculations also suggest the possibility of the hybrid distal-to-alternating pathway which may operate during the nitrogen reduction process. In addition, interconversion of the isomeric nitrogenous species involved in the alternating (**[5]$_{alt}$**, **[6]$_{alt}$** and **[7]$_{alt}$**) and distal (**[5]$_{dis}$**, **[6]$_{dis}$** and **[7c]$_{dis}$**) pathways is unlikely to occur. The calculated reaction free energies of different steps as well as the lower barrier heights of the transition states (TSs) involved in the catalytic cycle demonstrated their potential towards dinitrogen activation process.

[1.8] Bibliography

[1] Jensen, F. (2017). *Introduction to Computational Chemistry*. John wiley & sons.

[2] Lewars, E. (2008).*Computational Chemistry: Introduction to the Theory and Applications of Molecular and Quantum mechanics*. Springer (India) Pvt. Ltd., New Delhi, 2nd Edition.

[3] (a) Parr, R. G. and Yang, W. (1989). *Density Functional Theory of Atoms and Molecules*. Oxford University Press, Oxford, New York; (b) Koch, W. and Holthausen, M. C. (2000) *A Chemist's Guide to Density Functional Theory*. Wiley-VCH, Weinheim; (c) Hohenberg, P. and Kohn, W. Inhomogeneous Electron Gas. *Physical Review B*, 136(3):864, 1964; (d) Kohn, W., and Sham, L. J. Self-Consistent Equations Including Exchange and Correlation Effects. *Physical Review A*, 140(4): 1133, 1965; (e) Kohn, W., Becke, A. D., and Parr, R. G. Density Functional Theory of Electronic Structure. *The Journal of Physical Chemistry*, 100(31):12974-12980, 1996; (f) Baerends, E. J., and Gritsenko, O. V. A Quantum Chemical View of Density Functional Theory. *The Journal of Physical Chemistry A*, 101(30):5383-5403.

[4] Slater, J. C. Comparison of TFD and Xα methods for molecules and solids. *International Journal of Quantum Chemistry*, 9(S9):7-21, 1975.

[5] Johnson, K. H. (1973). Scattered-wave theory of the chemical bond. In *Advances in quantum chemistry*, Volume. 7, pages- 143-185, Academic Press.

[6] Heine, V. (1975). Solid State and Molecular Theory: A Scientific Biography, Wiley, New York.

[7] Lee, C., Yang, W., and Parr, R. G. Development of the Colle-Salvetti Correlation-Energy Formula Into a Functional of the Electron Density. *Physical Review B*, 37(2):785-789, 1988.

[8] Becke, A. D. Density-Functional Exchange-Energy Approximation with Correct Asymptotic Behavior. *Physical Review A*, 38(6):3098-3100, 1988.

[9] Perdew, J. P., Burke, K., and Wang, Y. Generalized Gradient Approximation for the Exchange-Correlation Hole of a Many-Electron System. *Physical Review B*, 54(23):16533-16539, 1996.

[10] Tao, J., Perdew, J. P., Staroverov, V. N., and Scuseria, G. E. Climbing the Density Functional Ladder: Nonempirical Meta–Generalized Gradient Approximation Designed for Molecules and Solids. *Physical Review Letters*, 91(14):146401, 2003.

[11] Rey, J., and Savin, A. Virtual space level shifting and correlation energies. *International Journal of Quantum Chemistry*, 69(4):581–590, 1998

[12] Zhao, Y. and Truhlar, D. G. A New Local Density Functional for Main- Group Thermochemistry, Transition Metal Bonding, Thermochemical Kinetics, and Noncovalent Interactions. *The Journal of Chemical Physics*, 125(19):194101, 2006.

[13] Stephens, P. J., Devlin, F. J., Chabalowski, C. F. N., and Frisch, M. J. Ab initio calculation of vibrational absorption and circular dichroism spectra using density functional force fields. *The Journal of Physical Chemistry*, 98(45):11623–11627, 1994.

[14] Grimme, S. Semiempirical hybrid density functional with perturbative second-order correlation. *The Journal of Chemical Physics*, 124(3):034108, 2006.

[15] Boys, S. F. Electronic Wave Functions-I. A General Method of Calculation for the Stationary States of Any Molecular System. *Proceedings of the Royal Society A*, 200(1063):542-554, 1950.

[16] Slater, J. C. Atomic Shielding Constants. *Physical Review*, 36(1):57-64, 1930.

[17] Hehre, W. J., Stewart, R. F., and Pople, J. A. Self-consistent molecular-orbital methods. I. Use of gaussian expansions of Slater-type atomic orbitals. *The Journal of Chemical Physics*, 51(6):2657–2664, 1969.

[18] Binkley, J. S., Pople, J. A., and Hehre, W. J. Self-consistent molecular orbital methods. 21. Small split-valence basis sets for first-row elements. *Journal of the American Chemical Society*, 102(3):939–947, 1980.

[19] (a) Frisch, M. J., Pople, J. A., and Binkley, J. S. Self-consistent molecular orbital methods 25. Supplementary functions for Gaussian basis sets. *The Journal of Chemical Physics*, 80(7):3265-3269, 1984; (b) Hehre, W. J., Ditchfield, R., and Pople, J. A. Self—consistent molecular orbital methods. XII. Further extensions of Gaussian—type basis sets for use in molecular orbital studies of organic molecules. *The Journal of Chemical Physics*, 56(5):2257-2261, 1972

[20] Ditchfield, R. H. W. J., Hehre, W. J., and Pople, J. A. Self-consistent molecular-orbital methods. IX. An extended Gaussian-type basis for molecular-orbital studies of organic molecules. *The Journal of Chemical Physics*, 54(2):724–728, 1971

[21] (a) McLean, A. D., and Chandler, G. S. Contracted Gaussian basis sets for molecular calculations. I. Second row atoms, Z= 11–18. *The Journal of Chemical Physics*, 72(10):5639–5648, 1980; (b) Krishnan, R. B. J. S., Binkley, J. S., Seeger, R., and Pople,

J. A. Self-consistent molecular orbital methods. XX. A basis set for correlated wave functions. *The Journal of Chemical Physics*, 72(1):650–654, 1980

[22] Frenking, G., Antes, I., Böhme, M., Dapprich, S., Ehlers, A. W., Jonas, V., Neuhaus, A., Otto, M., Stegmann, R., Veldkamp, A., and Vyboishchikov, S. F. Pseudopotential Calculations of Transition Metal Compounds: Scope and Limitations. *Reviews in Computational Chemistry*, 8:63-144, 2007.

[23] (a) Hay, P. J. and Wadt, W. R. Ab initio effective core potentials for molecular calculations. Potentials for the transition metal atoms Sc to Hg. *The Journal of Chemical Physics*, 82(1):270–283, 1985; (b) Wadt, W. R. and Hay, P. J. Ab initio effective core potentials for molecular calculations. Potentials for main group elements Na to Bi. *The Journal of Chemical Physics*, 82(1):284–298, 1985; (c) Hay, P. J. and Wadt, W. R. Ab initio effective core potentials for molecular calculations. Potentials for K to Au including the outermost core orbitals. *The Journal of Chemical Physics*, 82(1):299–310, 1985.

[24] (a) Fuentealba, P., Preuss, H., Stoll, H., and Von Szentpály, L. A proper account of core-polarization with pseudopotentials: single valence-electron alkali compounds. *Chemical Physics Letters*, 89(5):418–422, 1982; (b) Von Szentpály, L., Fuentealba, P., Preuss, H., and Stoll, H. Pseudopotential calculations on Rb^{+}_{2}, Cs^{+}_{2}, RbH^{+}, CsH^{+} and the mixed alkali dimer ions. *Chemical Physics Letters*, 93(6):555–559, 1982; (c) Fuentealba, P., Stoll, H., Von Szentpaly, L., Schwerdtfeger, P., and Preuss, H. On the reliability of semi-empirical pseudopotentials: simulation of Hartree-Fock and Dirac-Fock results. *Journal of Physics B: Atomic and Molecular Physics*, 16(11):L323, 1983.

[25] (a) Douglas, M., and Kroll, N. M. Quantum electrodynamical corrections to the fine structure of helium. *Annals of Physics*, 82(1):89-155, 1974; (b) Hess, B. A. Applicability of the no-pair equation with free-particle projection operators to atomic and molecular structure calculations. *Physical Review A*, 32(2):756, 1985; (c) Hess, B. A. Relativistic electronic-structure calculations employing a two-component no-pair formalism with external-field projection operators. *Physical Review A*, 33(6):3742, 1986.

[26] (a) Pizlo, A., Jansen, G., Heß, B. A., and Von Niessen, W. Ionization potential and electron affinity of the Au atom and the AuH molecule by all-electron relativistic configuration interaction and propagator techniques. *The Journal of chemical physics*, 98(5):3945-3951, 1993; (b) Hess, B. A., and Kaldor, U. Relativistic all-electron coupled-cluster calculations on Au_2 in the framework of the Douglas–Kroll transformation. *The Journal of Chemical Physics*, 112(4):1809-1813, 2000.

[27] Bader, R. F. W. A Quantum Theory of Molecular Structure and Its Applications. *Chemical Reviews*, 91(5):893-928, 1991.

[28] Lu, T., and Chen, F. Multiwfn: A multifunctional wavefunction analyzer. *Journal of Computational Chemistry*, 33(5):580-592, 2012.

[29] Cremer, D., and Kraka, E. Chemical Bonds Without Bonding Electron Density—Does the Difference Electron-Density Analysis Suffice for a Description of the Chemical Bond? *Angewandte Chemie International Edition in English*, 23(8):627-628, 1984.

[30] (a) Zhao, L., von Hopffgarten, M., Andrada, D. M., and Frenking, G. Energy Decomposition Analysis. *Wiley Interdisciplinary Reviews: Computational Molecular Science*, 8(3):e1345, 2018; (b) Mitoraj, M. P., Michalak, A., and Ziegler, T. A Combined Charge and Energy Decomposition Scheme for Bond Analysis. *Journal of Chemical Theory and Computation*, 5(4):962-975, 2009.

[31] Fernández, I., and Bickelhaupt, F. M. The activation strain model and molecular orbital theory: understanding and designing chemical reactions. *Chemical Society Reviews*, 43(14):4953-4967, 2014.

[32] Ess, D. H., and Houk, K. N. Distortion/Interaction Energy Control of 1,3-Dipolar Cycloaddition Reactivity. *Journal of the American Chemical Society*, 129(35):10646-10647, 2007.

[33] van Zeist, W. J., and Bickelhaupt, F. M. The activation strain model of chemical reactivity. *Organic & biomolecular chemistry*, 8(14):3118-3127, 2010.

[34] Hopkinson, M. N., Richter, C., Schedler, M., and Glorius, F. An overview of N-heterocyclic carbenes. *Nature*, 510(7506):485-496, 2014.

[35] Nolan, S. P. The Development and Catalytic Uses of *N*-Heterocyclic Carbene Gold Complexes. *Accounts of Chemical Research*, 44(2):91-100, 2011.

[36] Vougioukalakis, G. C., and Grubbs, R. H. Ruthenium-Based Heterocyclic Carbene-Coordinated Olefin Metathesis Catalysts. *Chemical Reviews*, 110(3):1746-1787, 2010.

[37] Allen, W. D., and Schaefer III, H. F. Geometrical structures, force constants, and vibrational spectra of SiH, SiH_2, SiH_3, and SiH_4. *Chemical Physics*, 108(2):243-274, 1986.

[38] Balasubramanian, K., and McLean, A. D. The singlet–triplet energy separation in silylene. *The Journal of Chemical Physics*, 85(9):5117-5119, 1986.

[39] Arduengo III, A. J., Harlow, R. L., and Kline, M. A Stable Crystalline Carbene. *Journal of the American Chemical Society*, 113(1):361-363, 1991.

[40] Dröge, T., and Glorius, F. The Measure of All Rings—*N*-Heterocyclic Carbenes. *Angewandte Chemie International Edition*, 49(39):6940-6952, 2010.

[41] Frémont, de P., Marion N., and Nolan, S. P. Carbenes: Synthesis, properties, and organometallic chemistry, *Coordination Chemistry Reviews*, 253(7-8):862–892, 2009.

[42] Hahn, F. E., and Jahnke, M. C. Heterocyclic Carbenes: Synthesis and Coordination Chemistry. *Angewandte Chemie International Edition*, 47(17):3122-3172, 2008.

[43] Wanzlick, H. W., and Schönherr, H. J. Direct Synthesis of a Mercury Salt-Carbene Complex. *Angewandte Chemie International Edition in English*, 7(2):141-142, 1968.

[44] Hitchcock, P. B., Lappert M. F., and Pye, P. L. Carbene Complexes. Part 14. The Synthesis and Steric and Electronic Effects in Electron-rich Olefin-derived Bis-, Tris-, and Tetrakis-(Carbene)-ruthenium(II) and a Tetrakis (carbene)osmium(II) Complex; the Crystal and Molecular Structure of *trans*-Dichiorotetrakis(1, 3-diethylimidazo-lidin-2-ylidene)ruthenium(II). *Journal of the Chemical Society, Dalton Transactions,* (7):826–836,1978.

[45] M. J. Doyle and M. F. Lappert, Activation Parameters for Rotation about an M–C_{carb} Bond from Temperature Dependent ^{1}H N.m.r. Spectra of Rh^{I} Carbene Complexes. *Journal of the Chemical Society, Chemical Communications*, (17):679–680, 1974.

[46] Lappert, M. F., and Maskell, R. K. Homogeneous catalysis: VIII. Carbene-transition-metal complexes as hydrosilylation catalysts. *Journal of Organometallic Chemistry*, 264(1-2):217-228, 1984.

[47] Öfele, K. 1, 3-Dimethyl-4-imidazolinyliden-(2)-pentacarbonylchrom ein neuer Übergangsmetall-carben-komplex. *Journal of Organometallic Chemistry*, 12(3):P42-P43, 1968.

[48] Martin, D., Baceiredo, A., Gornitzka, H., Schoeller, W. W., and Bertrand, G. A Stable P-Heterocyclic Carbene. *Angewandte Chemie International Edition*, 44(11):1700-1703, 2005.

[49] Masuda, J. D., Martin, D., Lyon-Saunier, C., Baceiredo, A., Gornitzka, H., Donnadieu. B., and Bertrand, G. Stable P-Heterocyclic Carbenes: Scope and Limitations, Chemistry–An Asian Journal, 2(1):178-187, 2007.

[50] Ruiz, J., and Perandones, B. F. Metal-induced tautomerization of oxazole and thiazole molecules to heterocyclic carbenes. *Chemical Communications*, (19):2741-2743, 2009.

[51] Vougioukalakis, G. C., and Grubbs, R. H. Synthesis and Activity of Ruthenium Olefin Metathesis Catalysts Coordinated with Thiazol-2-ylidene Ligands. *Journal of the American Chemical Society*, 130(7):2234-2245, 2008.

[52] Raubenheimer, H. G., and Cronje, S. Carbene complexes derived from lithiated heterocycles, mainly azoles, by transmetallation. *Journal of Organometallic Chemistry*, 617-618:170-181, 2001.

[53] Raubenheimer, H. G., Stander, Y., Marais, E. K., Thompson, C., Kruger, G. J., Cronje, S., and Deetlefs, M. Group 6 carbene complexes derived from lithiated azoles and the crystal structure of a molybdenum thiazolinylidene complex. *Journal of Organometallic Chemistry*, 590(2):158-168, 1999.

[54] Gründemann, S., Kovacevic, A., Albrecht, M., Robert, J. W. F., and Crabtree, H. Abnormal binding in a carbene complex formed from an imidazolium salt and a metal hydride complex. *Chemical Communications*, (21):2274-2275, 2001.

[55] Gruendemann, S., Kovacevic, A., Albrecht, M., Faller, J. W., and Crabtree, R. H. Abnormal Ligand Binding and Reversible Ring Hydrogenation in the Reaction of Imidazolium Salts with $IrH_5(PPh_3)_2$. *Journal of the American Chemical Society*, 124(35):10473-10481, 2002.

[56] Mathew, P., Neels, A., and Albrecht, M. 1, 2, 3-Triazolylidenes as Versatile Abnormal Carbene Ligands for Late Transition Metals. *Journal of the American Chemical Society*, 130(41):13534-13535, 2008.

[57] Guisado-Barrios, G., Bouffard, J., Donnadieu, B., and Bertrand, G. Crystalline 1*H*-1, 2, 3-Triazol-5-ylidenes: New Stable Mesoionic Carbenes (MICs). *Angewandte Chemie International Edition*, 49(28):4759-4762, 2010.

[58] Arduengo III, A. J., Goerlich, J. R., and Marshall, W. J. A Stable Diaminocarbene. *Journal of the American Chemical Society*, 117(44):11027-11028, 1995.

[59] Gusev, D. G. Electronic and Steric Parameters of 76 N-Heterocyclic Carbenes in $Ni(CO)_3(NHC)$. *Organometallics*, 28(22):6458-6461, 2009.

[60] Iglesias, M., Beetstra, D. J., Stasch, A., Horton, P. N., Hursthouse, M. B., Coles, S. J., Cavell, K.J., Dervisi, A., and Fallis, I. A. First Examples of Diazepanylidene Carbenes and Their Late-Transition-Metal Complexes. *Organometallics*, 26(19):4800-4809, 2007.

[61] Scarborough, C. C., Guzei, I. A., and Stahl, S. S. Synthesis and isolation of a stable, axially-chiral seven-membered *N*-heterocyclic carbene. *Dalton Transactions*, (13):2284-2286, 2009.

[62] Iglesias, M., Beetstra, D. J., Knight, J. C., Ooi, L. L., Stasch, A., Coles, S., Male, L., Hursthouse, M. B., Cavell, K. J., Dervisi, A. and Fallis, I. A. Novel Expanded Ring N-Heterocyclic Carbenes: Free Carbenes, Silver Complexes, and Structures. *Organometallics*, 27(13):3279-3289, 2008.

[63] Ruiz, J., García, L., Perandones, B. F., and Vivanco, M. A Fischer carbene within an Arduengo carbene. *Angewandte Chemie International Edition*, 50(13):3010-3012, 2011.

[64] Ruiz, J., García, L., Mejuto, C., Vivanco, M., Díaz, M. R., and García-Granda, S. Strong electron-donating metalla-N-heterocyclic carbenes. *Chemical Communications*, 50(17):2129-2132, 2014.

[65] Ruiz, J., García, L., Vivanco, M., Berros, Á., and Van der Maelen, J. F. Generating and Trapping Metalla-N-Heterocyclic Carbenes. *Angewandte Chemie International Edition*, 54(14):4212-4216, 2015.

[66] Ernzerhof, M., and Scuseria, G. E. Assessment of the Perdew–Burke–Ernzerhof exchange-correlation functional. *The Journal of Chemical Physics*, 110(11):5029-5036, 1999.

[67] Adamo, C., and Barone, V. Toward reliable density functional methods without adjustable parameters: The PBE0 model. *The Journal of Chemical Physics*, 110(13):6158-6170, 1999.

[68] Francl, M. M., Pietro, W. J., Hehre, W. J., Binkley, J. S., Gordon, M. S., DeFrees, D. J., and Pople, J. A. Self-consistent molecular orbital methods. XXIII. A polarization-type basis set for second-row elements. *The Journal of Chemical Physics*, 77(7):3654-3665, 1982.

[69] Rassolov, V. A., Pople, J. A., Ratner, M. A., and Windus, T. L. 6-31G* basis set for atoms K through Zn. *The Journal of Chemical Physics*, 109(4):1223-1229, 1998.

[70] Rassolov, V. A., Ratner, M. A., Pople, J. A., Redfern, P. C., and Curtiss, L. A. 6-31G* basis set for third-row atoms. *Journal of Computational Chemistry*, 22(9):976-984, 2001.

[71] Ceolin, G. A., de Berrêdo, R. C., and Jorge, F. E. Gaussian basis sets of quadruple zeta quality for potassium through xenon: application in CCSD(T) atomic and molecular property calculations. *Theoretical Chemistry Accounts*, 132:1339, 2013.

[72] Jansen, G., and Hess, B. A. Revision of the Douglas-Kroll transformation. *Physical Review A*, 39(11):6016, 1989.

[73] Zhao, Y., and Truhlar, D. G. The M06 suite of density functionals for main group thermochemistry, thermochemical kinetics, noncovalent interactions, excited states, and transition elements: two new functionals and systematic testing of four M06-class functionals and 12 other functionals. *Theoretical Chemistry Accounts*, 120(1):215-241, 2008.

[74] Weigend, F., and Ahlrichs, R. Balanced basis sets of split valence, triple zeta valence and quadruple zeta valence quality for H to Rn: Design and assessment of accuracy. *Physical Chemistry Chemical Physics*, 7(18):3297-3305, 2005.

[75] Weigend, F. Accurate Coulomb-fitting basis sets for H to Rn. *Physical Chemistry Chemical Physics*, 8(9):1057-1065, 2006.

[76] Denk, M., Lennon, R., Hayashi, R., West, R., Belyakov, A. V., Verne, H. P., Haaland, A., Wagner, M., and Metzler, N. Synthesis and Structure of a Stable Silylene. *Journal of the American Chemical Society*, 116(6):2691-2692, 1994.

[77] Meller, A., and Gräbe, C. P. Synthese und Isolierung neuer Germanium(II)-Verbindungen und freier Germylene. *Chemische Berichte*, 118(5):2020-2029, 1985.

[78] (a) Gaspar, P. P., Xiao, M., Pae, D. H., Berger, D. J., Haile, T., Chen, T., Lei, D., Winchester, W. R., and Jiang, P. The quest for triplet ground state silylenes. *Journal of Organometallic Chemistry*, 646(1-2):68-79, 2002; (b) Lee, V. Y., and Sekiguchi, A. (2010). *Organometallic Compounds of Low-Coordinate Si, Ge, Sn and Pb: From Phantom Species to Stable Compounds*, John Wiley & Sons, pages.139-197.

[79] (a) Gehrhus, B., and Lappert, M. F. Chemistry of thermally stable bis(amino)silylenes. *Journal of Organometallic Chemistry*, 617-618:209-223, 2001; (b) Gehrhus, B., Lappert, M. F., Heinicke, J., Boese, R., and Bläser, D. Synthesis, structures and reactions of new thermally stable silylenes. *Journal of the Chemical Society, Chemical Communications*, (19):1931-1932, 1995.

[80] Kosai, T., Ishida, S., and Iwamoto, T. A Two-Coordinate Cyclic (Alkyl)(amino)silylene: Balancing Thermal Stability and Reactivity. *Angewandte Chemie International Edition*, 55(50):15554-15558, 2016.

[81] Wang, L., Lim, Y. S., Li, Y., Ganguly, R., and Kinjo, R. Isolation of a Cyclic (Alkyl)(amino)germylene. *Molecules*, 21(8):990, 2016.

[82] Lavallo, V., Canac, Y., Präsang, C., Donnadieu, B., and Bertrand, G. Stable Cyclic (Alkyl)(Amino) Carbenes as Rigid or Flexible, Bulky, Electron-Rich Ligands for Transition-Metal Catalysts: A Quaternary Carbon Atom Makes the Difference. *Angewandte Chemie International Edition*, 44(35):5705-5709, 2005.

[83] Koike, T., Kosai, T., and Iwamoto, T. 1, 4-Dehydrogenation with a Two-Coordinate Cyclic (Alkyl)(amino)silylene. *Chemistry–A European Journal*, 25(39):9295-9302, 2019.

[84] Cui, C., Roesky, H. W., Schmidt, H. G., Noltemeyer, M., Hao, H., and Cimpoesu, F. Synthesis and Structure of a Monomeric Aluminum(I) Compound [{HC(CMeNAr)$_2$}Al](Ar= 2,6–^{i}Pr$_2$C$_6$H$_3$): A Stable Aluminum Analogue of a Carbene. *Angewandte Chemie International Edition*, 39(23):4274-4276, 2000.

[85] Hardman, N. J., Eichler, B. E., and Power, P. P. Synthesis and characterization of the monomer Ga{(NDippCMe)$_2$CH}(Dipp=C$_6$H$_3$Pr$^{i}_2$-2,6): a low valent gallium(I) carbene analogue. *Chemical Communications*, (20):1991-1992, 2000.

[86] Hill, M. S., and Hitchcock, P. B. A mononuclear indium(I) carbene analogue. *Chemical Communications*, (16):1818-1819, 2004.

[87] Hill, M. S., Hitchcock, P. B., and Pongtavornpinyo, R. Neutral carbene analogues of the heaviest Group 13 elements: Consideration of electronic and steric effects on structure and stability. *Dalton Transactions*, (2):273-277, 2005.

[88] Chu, T., and Nikonov, G. I. Oxidative Addition and Reductive Elimination at Main-Group Element Centers. *Chemical Reviews*, 118(7):3608-3680, 2018.

[89] Asay, M., Jones, C., and Driess, M. *N*-Heterocyclic Carbene Analogues with Low-Valent Group 13 and Group 14 Elements: Syntheses, Structures, and Reactivities of a New Generation of Multitalented Ligands. *Chemical Reviews*, 111(2):354-396, 2011.

[90] Chang, M. C., and Otten, E. Reduction of (Formazanate) boron Difluoride Provides Evidence for an *N*-Heterocyclic B(I) Carbenoid Intermediate. *Inorganic Chemistry*, 54(17):8656-8664, 2015.

[91] Bharadwaz, P., and Phukan, A. K. Introducing *N*-Heterocyclic Borylenes: Theoretical Prediction of Stable, Neutral, Monomeric Boron(I) Carbenoids. *Inorganic Chemistry*, 58(9):5428-5432, 2019.

[92] Nakafuji, S. Y., Kobayashi, J., and Kawashima, T. Generation and Coordinating Properties of a Carbene Bearing a Phosphorus Ylide: An Intensely Electron-Donating Ligand. *Angewandte Chemie International Edition*, 47(6):1141-1144, 2008.

[93] Fürstner, A., Alcarazo, M., Radkowski, K., and Lehmann, C. W. Carbenes Stabilized by Ylides: Pushing the Limits. *Angewandte Chemie International Edition*, 47(43):8302-8306, 2008.

[94] Borthakur, B., and Phukan, A. K. Moving toward Ylide-Stabilized Carbenes. *Chemistry–A European Journal*, 21(32):11603-11609, 2015.

[95] Asay, M., Inoue, S., and Driess, M. Aromatic Ylide-Stabilized Carbocyclic Silylene. *Angewandte Chemie International Edition*, 50(41):9589-9592, 2011.

[96] Alvarado-Beltran, I., Baceiredo, A., Saffon-Merceron, N., Branchadell, V., and Kato, T. Cyclic Amino(Ylide)Silylene: A Stable Heterocyclic Silylene with Strongly Electron-Donating Character. *Angewandte Chemie International Edition*, 55(52):16141-16144, 2016.

[97] Berthe, J., Garcia, J. M., Ocando, E., Kato, T., Saffon-Merceron, N., De Cózar, A., Cossío, F. P., and Baceiredo, A. Synthesis and Reactivity of a Phosphine-Stabilized Monogermanium Analogue of Alkynes. *Journal of the American Chemical Society*, 133(40):15930-15933, 2011.

[98] Sarbajna, A., Swamy, V. S. V. S. N., and Gessner, V. H. Phosphorus-ylides: powerful substituents for the stabilization of reactive main group compounds. *Chemical Science*, 12(6):2016-2024, 2021.

[99] Parkin, G. A Simple Description of the Bonding in Transition-Metal Borane Complexes. *Organometallics*, 25(20):4744-4747, 2006.

[100] Hill, A. F. An Unambiguous Electron-Counting Notation for Metallaboratranes. *Organometallics*, 25(20):4741-4743, 2006.

[101] Anderson, J. S., Rittle, J., and Peters, J. C. Catalytic conversion of nitrogen to ammonia by an iron model complex. *Nature*, 501(7465):84-87, 2013.

[102] Rudd, P. A., Planas, N., Bill, E., Gagliardi, L., and Lu, C. C. Dinitrogen Activation at Iron and Cobalt Metallalumatranes. *European Journal of Inorganic Chemistry*, 2013(22-23):3898-3906, 2013.

[103] Clouston, L. J., Bernales, V., Carlson, R. K., Gagliardi, L., and Lu, C. C. Bimetallic Cobalt–Dinitrogen Complexes: Impact of the Supporting Metal on N_2 Activation. *Inorganic Chemistry*, 54(19):9263-9270, 2015.

[104] Takaya, J., and Iwasawa, N. Synthesis, Structure, and Catalysis of Palladium Complexes Bearing a Group 13 Metalloligand: Remarkable Effect of an Aluminum-Metalloligand in Hydrosilylation of CO_2. *Journal of the American Chemical Society*, 139(17):6074-6077, 2017.

[105] Cammarota, R. C., Vollmer, M. V., Xie, J., Ye, J., Linehan, J. C., Burgess, S. A., Appel, A. M., Gagliardi, L., Lu, C. C. A Bimetallic Nickel–Gallium Complex Catalyzes CO_2 Hydrogenation via the Intermediacy of an Anionic d^{10} Nickel Hydride. *Journal of the American Chemical Society*, 139(40):14244-14250, 2017.

[106] Cammarota, R. C., and Lu, C. C. Tuning Nickel with Lewis Acidic Group 13 Metalloligands for Catalytic Olefin Hydrogenation. *Journal of the American Chemical Society*, 137(39):12486-12489, 2015.

[107] Nesbit, M. A., Suess, D. L., and Peters, J. C. E–H Bond Activations and Hydrosilylation Catalysis with Iron and Cobalt Metalloboranes. *Organometallics*, 34(19):4741-4752, 2015.

[108] Harman, W. H., Lin, T. P., and Peters, J. C. A d^{10} Ni–(H_2) Adduct as an Intermediate in H–H Oxidative Addition across a Ni–B Bond. *Angewandte Chemie International Edition*, 53(4):1081-1086, 2014.

[109] Harman, W. H., and Peters, J. C. Reversible H_2 Addition across a Nickel–Borane Unit as a Promising Strategy for Catalysis. *Journal of the American Chemical Society*, 134(11):5080-5082, 2012.

[110] Suess, D. L., and Peters, J. C. H–H and Si–H Bond Addition to Fe≡NNR_2 Intermediates Derived from N_2. *Journal of the American Chemical Society*, 35(13):4938-4941, 2013.

[111] Zeng, G., and Sakaki, S. Unexpected Electronic Process of H_2 Activation by a New Nickel Borane Complex: Comparison with the Usual Homolytic and Heterolytic Activations. *Inorganic Chemistry*, 52(6):2844-2853, 2013.

[112] Cammarota, R. C., Xie, J., Burgess, S. A., Vollmer, M. V., Vogiatzis, K. D., Ye, J., Linehan, J. C., Appel, A. M., Hoffmann, C., Wang, X., Yong, Jr, V. G, and Lu, C. C. Thermodynamic and kinetic studies of H_2 and N_2 binding to bimetallic nickel-group 13 complexes and neutron structure of a Ni (η^2-H_2) adduct. *Chemical Science*, 10(29):7029-7042, 2019.

[113] Huheey, J. E., Keiter, E. A., and Keiter, R. L. (1993) *Inorganic Chemistry: Principles of Structure and Reactivity*. Harper Collins College Publishers, New York.

[114] Jennings, J. R. (1991) *Catalytic Ammonia Synthesis: Fundamentals and Practice*. Springer Science & Business Media,

[115] Schlögl, R. (2008) Ammonia Synthesis. In, *Handbook of Heterogeneous Catalysis*, of, pages 2501-2575, 3527312412. Wiley-VCH.

[116] Hoffman, B. M., Lukoyanov, D., Yang, Z.-Y., Dean, D. R., and Seefeldt, L. C. Mechanism of Nitrogen Fixation by Nitrogenase: The Next Stage. *Chemical Reviews*, 114(8):4041-4062, 2014.

[117] Kirn, J. and Rees, D. Crystallographic structure and functional implications of the nitrogenase molybdenum–iron protein from Azotobacter vinelandii. *Nature*, 360(6404):553-560, 1992.

[118] Lancaster, K. M., Roemelt, M., Ettenhuber, P., Hu, Y., Ribbe, M. W., Neese, F., Bergmann, U., and DeBeer, S. X-ray Emission Spectroscopy Evidences a Central Carbon in the Nitrogenase Iron-Molybdenum Cofactor. *Science*, 334(6058):974-977, 2011.

[119] Chalkley, M. J., Drover, M. W., and Peters, J. C. Catalytic N_2-to-NH_3 (or-N_2H_4) Conversion by Well-Defined Molecular Coordination Complexes. *Chemical Reviews*, 120(12):5582-5636, 2020.

[120] Scheibel, M. G. and Schneider, S. New Insights into the Biological and Synthetic Fixation of Nitrogen. *Angewandte Chemie International Edition*, 51(19):4529-4531, 2012.

[121] Tanabe, Y. and Nishibayashi, Y. Comprehensive insights into synthetic nitrogen fixation assisted by molecular catalysts under ambient or mild conditions. *Chemical Society Reviews*, 50(8):5201-5242, 2021.

[122] Nishibayashi, Y. Development of catalytic nitrogen fixation using transition metal–dinitrogen complexes under mild reaction conditions. *Dalton Transactions*, 47(33):11290-11297, 2018.

[123] Yandulov, D. V. and Schrock, R. R. Catalytic Reduction of Dinitrogen to Ammonia at a Single Molybdenum Center. *Science*, 301(5629):76-78, 2003.

[124] Schrock, R. R. Catalytic Reduction of Dinitrogen to Ammonia by Molybdenum: Theory Versus Experiment. *Angewandte Chemie International Edition*, 47(30):5512-5522, 2008.

[125] Yandulov, D. V. and Schrock, R. R. Studies Relevant to Catalytic Reduction of Dinitrogen to Ammonia by Molybdenum Triamidoamine Complexes. *Inorganic Chemistry*, 44(4):1103-1117, 2005.

[126] Schrock, R. R. Catalytic Reduction of Dinitrogen to Ammonia at a Single Molybdenum Center. *Accounts of Chemical Research*, 38(12):955-962, 2005.

[127] Studt, F. and Tuczek, F. Energetics and Mechanism of a Room-Temperature Catalytic Process for Ammonia Synthesis (Schrock Cycle): Comparison with Biological Nitrogen Fixation. *Angewandte Chemie International Edition*, 44(35):5639-5642, 2005.

[128] Arashiba, K., Miyake, Y., and Nishibayashi, Y. A molybdenum complex bearing PNP-type pincer ligands leads to the catalytic reduction of dinitrogen into ammonia. *Nature Chemistry*, 3(2):120-125, 2011.

[129] Eizawa, A., Arashiba, K., Tanaka, H., Kuriyama, S., Matsuo, Y., Nakajima, K., Yoshizawa, K., and Nishibayashi, Y. Remarkable catalytic activity of dinitrogen-bridged dimolybdenum complexes bearing NHC-based PCP-pincer ligands toward nitrogen fixation. *Nature Communications*, 8(1):1-12, 2017.

[130] Kuriyama, S. and Nishibayashi, Y. Development of catalytic nitrogen fixation using transition metal complexes not relevant to nitrogenases. *Tetrahedron*, 83:131986, 2021.

[131] Siedschlag, R. B., Bernales, V., Vogiatzis, K. D., Planas, N., Clouston, L. J., Bill, E., Gagliardi, L., and Lu, C. C. Catalytic Silylation of Dinitrogen with a Dicobalt Complex. *Journal of the American Chemical Society*, 137(14):4638-4641, 2015.

[132] Fajardo, J., Jr. and Peters, J. C. Catalytic Nitrogen-to-Ammonia Conversion by Osmium and Ruthenium Complexes. *Journal of the American Chemical Society*, 139(45):16105-16108, 2017.

[133] Tanabe, Y. and Nishibayashi, Y. Recent advances in nitrogen fixation upon vanadium complexes. *Coordination Chemistry Reviews*, 381:135-150, 2019.

[134] Zhao, Y., and Truhlar, D. G. A new local density functional for main-group thermochemistry, transition metal bonding, thermochemical kinetics, and noncovalent interactions. *The Journal of Chemical Physics*, 125(19):194101, 2006.